Hydrological Sciences Journal

ISSN: 0262-6667 (Print) 2150-3435 (Online) Journal homepage: https://www.tandfonline.com/loi/thsj20

Application of geochemical and stable isotopic tracers to investigate groundwater salinity in the Ochi-Narkwa Basin, Ghana

Samuel Y. Ganyaglo, Shiloh Osae, Tetteh Akiti, Thomas Armah, Laurence Gourcy, Tomas Vitvar, Mari Ito & Isaac A. Otoo

To cite this article: Samuel Y. Ganyaglo, Shiloh Osae, Tetteh Akiti, Thomas Armah, Laurence Gourcy, Tomas Vitvar, Mari Ito & Isaac A. Otoo (2017) Application of geochemical and stable isotopic tracers to investigate groundwater salinity in the Ochi-Narkwa Basin, Ghana, Hydrological Sciences Journal, 62:8, 1301-1316, DOI: 10.1080/02626667.2017.1322207

To link to this article: https://doi.org/10.1080/02626667.2017.1322207

View supplementary material

Published online: 22 May 2017.

Submit your article to this journal

Article views: 172

View Crossmark data

Citing articles: 3 View citing articles

Full Terms & Conditions of access and use can be found at
https://www.tandfonline.com/action/journalInformation?journalCode=thsj20

HYDROLOGICAL SCIENCES JOURNAL – JOURNAL DES SCIENCES HYDROLOGIQUES, 2017
VOL. 62, NO. 8, 1301–1316
https://doi.org/10.1080/02626667.2017.1322207

Check for updates

Application of geochemical and stable isotopic tracers to investigate groundwater salinity in the Ochi-Narkwa Basin, Ghana

Samuel Y. Ganyaglo[a,b], Shiloh Osae[a], Tetteh Akiti[b], Thomas Armah[c], Laurence Gourcy[d], Tomas Vitvar[e,f], Mari Ito[g] and Isaac A. Otoo[b]

[a]Nuclear Chemistry and Environmental Research Centre, Ghana Atomic Energy Commission/National Nuclear Research Institute, Legon-Accra, Ghana; [b]School of Nuclear and Allied Sciences (SNAS), University Of Ghana, Kwabenya, Ghana; [c]Department of Earth Science, University of Ghana, Legon, Accra, Ghana; [d]BRGM, Orleans, France; [e]Faculty of Environmental Science, Department of Applied Ecology, Czech University of Life Sciences, Prague, Czech Republic; [f]Faculty of Civil Engineering, Czech Technical University in Prague, Prague, Czech Republic; [g]Water Resources Programme, International Atomic Energy Agency, Vienna International Centre, Vienna, Austria

ABSTRACT

Rainwater, groundwater and soil-water samples were analysed to assess groundwater geochemistry and the origin of salinity in the Ochi-Narkwa basin of the Central Region of Ghana. The samples were measured for major ions and stable isotopes ($\delta^{18}O$, $\delta^{2}H$ and $\delta^{13}C$). The Cl^- content in rainwater decreased with distance from the coast. The major hydrochemical facies were Na-Cl for the shallow groundwaters and Ca-Mg-HCO_3, Na-Cl and Ca-Mg-Cl-SO_4 for the deep groundwaters. Groundwater salinization is caused largely by halite dissolution and to a minor extent by silicate weathering and seawater intrusion. Stable isotope composition of the groundwaters followed a slope of 3.44, suggesting a mixing line. Chloride profiles in the soil zone revealed the existence of salt crusts, which support halite dissolution in the study area. A conceptual flow model developed to explain the mechanism of salinization showed principal groundwater flow in the NW–SE direction.

ARTICLE HISTORY
Received 23 June 2015
Accepted 16 January 2017

EDITOR
D. Koutsoyiannis

ASSOCIATE EDITOR
K. Heal

KEYWORDS
geochemistry; stable isotopes; salinity sources; Ghana

1 Introduction

The growing interest in groundwater use in sub-Saharan Africa is prompted by the fact that surface water resources have been unable to satisfy the water demand for socio-economic development. In the past two decades, groundwater sources have become the preferred drinking water supply means to meet the growing demand of the largely rural and dispersed communities and small urban towns in Ghana. About 95% of groundwater use in Ghana is for household and drinking purposes. About 50% of the total number of hand-dug wells are used for drinking, whereas about 66% are used for both drinking and domestic purposes. Less than 5% of groundwater in Ghana is used for vegetable farming irrigation and livestock watering, mostly in the Volta, Upper East, Upper West and Greater Accra Regions (Obuobie and Barry 2010).

Groundwater is abstracted from all geological formations in the country. Kortatsi (1994) reported the existence of 56 000 groundwater abstraction systems consisting of boreholes, hand-dug wells and dugouts. Currently there are over 75 000 abstraction systems throughout the country. They include over 15 000 boreholes, 60 000 hand-dug wells and some dugouts. The aquifer yields are generally low, scarcely exceeding 6 m^3/h (Kortatsi 1994).

Groundwater quality in Ghana is generally considered to be good for domestic and agricultural purposes. However, reported low pH values (3.5–6.0), high iron concentrations (1–64 mg/L) and high salinity content (5000–14 584 mg/L) in some coastal aquifers (Kortatsi 1994) justify the need to investigate the hydro-geochemical and isotopic composition of groundwaters to understand the processes that contribute to elevated ionic concentrations in groundwater.

In the Ochi-Narkwa basin of the Central Region of Ghana, groundwater is an important source of potable water due to limited surface water supplies. It is used mainly for domestic purposes and, to a lesser extent, for industrial and agricultural purposes. One of the barriers to the exploitation of groundwater in the Central Region is poor water quality in the majority of the boreholes due to high salinity. The origin of the high salinity groundwaters in this area is still poorly

CONTACT Samuel Y. Ganyaglo sganyaglo@yahoo.co.uk; sganyaglo@gmail.com
Supplementary data for this article can be accessed here.
© 2017 IAHS

understood. Armah (2002) attributed the high salinity to multiple sources including seawater intrusion and mixing of freshwater with subsurface saline formation.

The use of chemical and isotopic tracers such as Br/Cl, $\delta^{18}O$, $\delta^{2}H$, ^{3}H, $^{87}Sr/^{86}Sr$, and $\delta^{11}B$ to determine the origin of salinity in groundwater has been demonstrated by various authors (Jørgensen and Banoeng-Yakubo 2001, Kim *et al.* 2003, Kortatsi 2006, Bouchaou *et al.* 2008). In this paper, chemical tracers (Br^{-}/Cl^{-}, Na^{+}/Cl^{-}, $SO4^{2-}/Cl^{-}$), stable oxygen and hydrogen isotopes ($\delta^{18}O$, $\delta^{2}H$) and carbon isotopes ($\delta^{13}C$) were employed to determine the origin of salinity in the coastal aquifers of the Central Region of Ghana, with a focus on the Ochi-Narkwa basin.

2 Study area

The study area lies between latitudes 5°11′45″–5°28.66′ 30″N and longitudes 0°33′41.6″–1°11′17″W and has a total area of 700 km^2, bounded to the south by the Gulf of Guinea (Fig. 1).

The prevailing climatic conditions in the area are dry equatorial and moist semi-equatorial. Annual rainfall ranges from 1000 mm along the coast to 2000 mm in the hinterland (Ghana Meteorological Agency, 2002–2011). The wettest months are May–June and September–October, whereas drier periods occur in December–February. The range of mean monthly minimum temperature is 22.8–24.9°C, whereas mean monthly maximum temperature is 27.2–31.9°C (Ghana Meteorological Agency, 2002–2011). The coldest month is August and the hottest months are March and April. The mean monthly relative humidity is 79–89% (Ghana Meteorological Agency, 2002–2011).

The largest part of the study area is drained by the River Ochi-Narkwa and its tributaries. It rises from the northern section of the study area, flows into the Narkwa Lagoon at the coast and discharges into the sea east of Narkwa village (Fig. 1). A small section of the study area is drained by the River Ayensu. The Ayensu basin drains a total area of 1709 km^2 and forms part of the Coastal River Basin System of Ghana. The source of this river is located in the Atewa hills in the East Akim District at an altitude of 610 m a.m.s.l.

The geology of the study area contains Paleoproterozoic Supracrustals and intrusive rocks constituting the Birimian Supergroup and rocks of the Eburnean Plutonic Suite (Fig. 2). The Birimian Supergroup consists of volcanic belts and sedimentary basins. The volcanic belts are composed of low-grade metamorphic tholeiitic basalts with intercalated volcaniclastics as well as minor andesitic and felsic flow rocks and local chemical sediments. The volcanic belts are intruded by coeval, comagmatic and synvolcanic granitoid plutons such as tonalite and granodiorite. The sedimentary basins comprise wacke and volcaniclastic sediments, mica schist, amphibolite of contact-metamorphic origin, biotite gneiss, locally migmatitic and minor biotite schist and undifferentiated

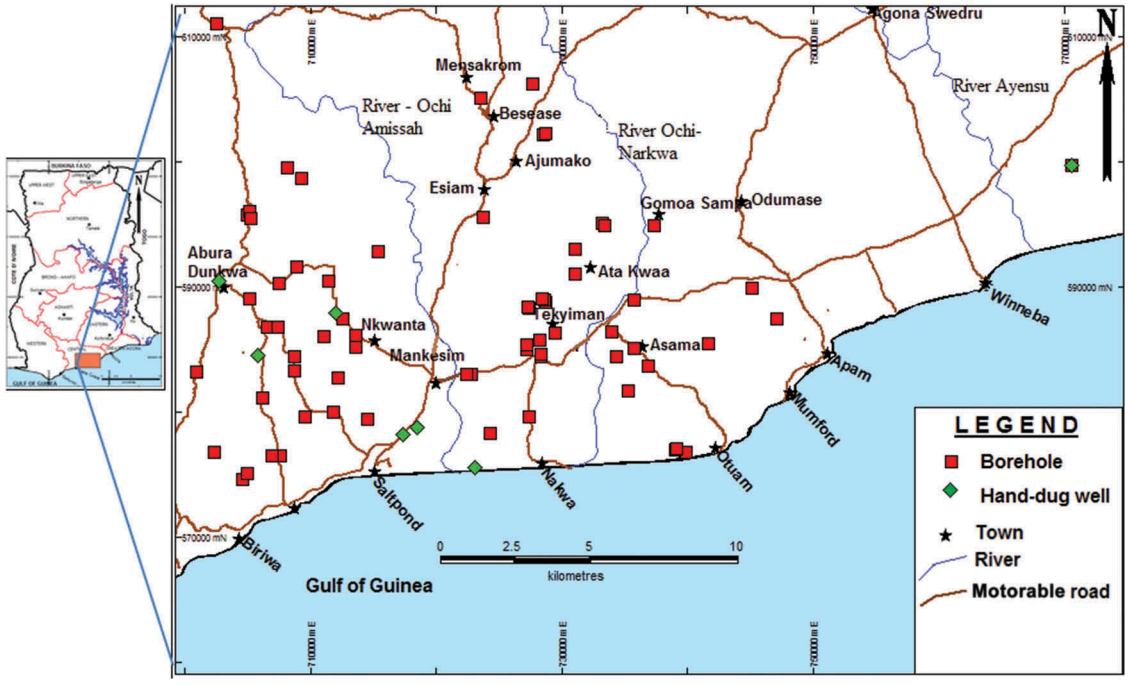

Figure 1. Location map of the study area with sampling points.

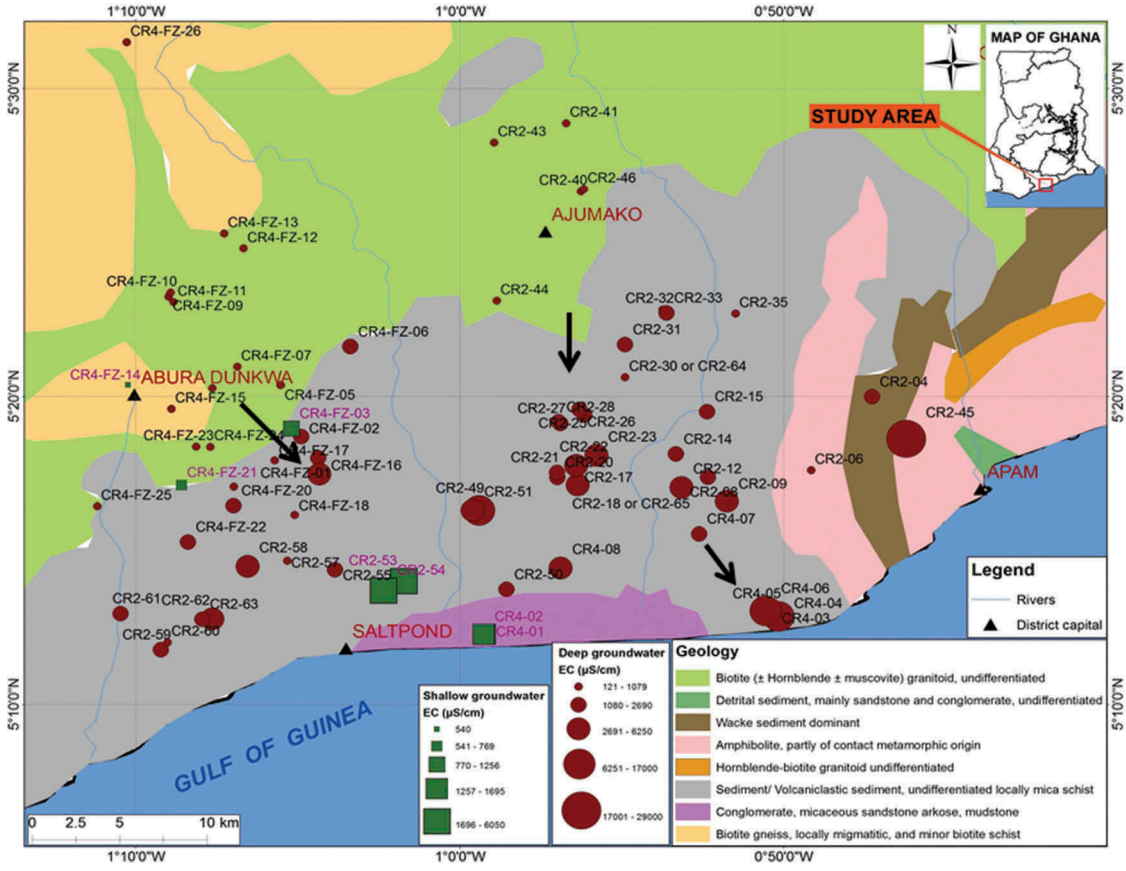

Figure 2. Geological map of the study area (modified from the New Geological Map of Ghana, Geological Survey Department of Ghana) showing spatial distribution of EC and inferred flow direction (→).

hornblende-biotite granitoid. The Eburnean Plutonic Suite consists of undifferentiated biotite granitoid, biotite gneiss and hornblende–biotite granitoid. Typical rock types in these groups have been reported (Leube *et al.* 1990, Hirdes *et al.* 1992, Taylor *et al.* 1992) as quartz diorites, tonalites and trondhjemites, granodiorites, adamellites and granites which intrude into the sedimentary basins. Part of the study area closer to the sea (Ekumfi Asafa area) falls within the Amisian group of the Mesozoic and includes conglomerates, mudstones, micaceous sandstones and arkoses (Fig. 2).

Groundwater is present in all principal lithologies in the area: sediment/volcaniclastic sediment, wacke sediment, biotite gneiss and biotite granitoid. Data held on 41 wells in the study area by the Community Water and Sanitation Agency (CWSA), Central Region, indicated that the thickness of the weathered zone varied from 0 to 30 m below the surface with a mean of 14.1 m. The borehole depth was 18–94.5 m with a mean of 34.5 m. The static water level varied from 0 to 20 m below the land surface. The mean static water level was 5.8 m. The borehole yield was 7.5–179.7 L/min and the mean yield was 32.1 L/min. The lowest yield of 7.5 L/min occurred in the schist aquifer; and the highest (179.7 L/min) occurred in the biotite gneiss/biotite granite contact in the Katakyiase area in the hinterland (Fig. 2). Of the boreholes, 52% were classified as confined and 48% as semi-confined. The transmissivity of the boreholes in the study area obtained from discharge and drawdown data ranged from 0.3 to 26.9 m^2/d, with a mean of 4.1 m^2/d for unconfined aquifers. In the case of confined aquifers the transmissivity values were 0.3–35.7 m^2/d. A hydraulic head map of the area showed that groundwater flows in the NW–SE direction, towards the coastline (Fig. 3).

3 Methods

A total of 78 water samples from 70 boreholes (deep wells, BH) and eight hand-dug wells (shallow wells, HD) were obtained. In total, 137 rainwater samples were collected at the Saltpond and Twifo Praso meteorological stations from 2010 to 2011 on an event basis. Thirty-five soil samples were obtained from four sites at various depths to assess the contribution of Cl^- in the soil to groundwater salinity. All water samples were collected in high-density polyethylene (HDPE) bottles,

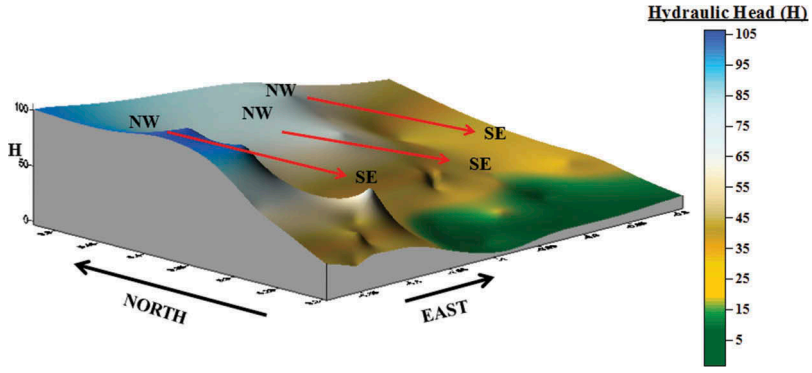

Figure 3. Hydraulic head (meters) map of the study area showing groundwater flow direction.

which were conditioned by washing initially with detergent, then with 10% nitric acid, and finally rinsing several times with distilled water. This was carried out to ensure that the sample bottles were free from contaminants. Representative *in situ* groundwater samples were collected after purging the aquifers to evacuate stagnant water in the borehole casing. Temperature, pH and redox potential (Eh) were measured in water samples in the field using a WTW 3110 field probe, and electrical conductivity (EC), total dissolved solids (TDS) and salinity were measured using a WTW 3210 field probe. Bicarbonates (HCO_3^-) were measured in the field by a titrimetric method as total alkalinity. Samples were filtered through 0.45-µm cellulose filters with the aid of a hand-operated vacuum pump. Part of the filtered water was used to rinse the sample bottles three times before sampling, as suggested by Boghici (2003). The remaining filtered water was then transferred into two 250-mL HDPE bottles for cation and anion analyses. The samples for cation analysis were acidified with 0.2M HNO_3 to preserve the ions in solution. Samples for stable isotope analysis were not filtered. The sample bottles (50-mL HDPE) were filled directly with the borehole water and then capped. The rainwater samples were collected from the rain gauges at the meteorological stations of Saltpond and Twifo Praso. Thirty-five soil samples from four profiles were collected by means of a hand auger. The samples were collected at 20-cm intervals to maximum depths of 160–200 cm and transferred into clean polyethylene zip-locked bags with a plastic trowel (IAEA 2008). The bags were immediately sealed, labelled and kept in ice chests at a relatively low temperature (4°C).

Chemical analyses of the water samples were carried out at the National Nuclear Research Institute (NNRI) of the Ghana Atomic Energy Commission (GAEC) using an atomic absorption spectrometer for calcium (Ca^{2+}), magnesium (Mg^{2+}) and trace metal determinations. Flame emission spectrometry was used for the measurement of sodium (Na^+) and potassium (K^+). A Dionex 90 ion chromatograph was used for the determination of Cl^-, SO_4^{2-}, Br^-, NO_3^-, PO_4^{3-} and F^-. A charge balance error of ±10% was accepted.

The Los Gatos Research (LGR) instrument, LGR DLT-100 (model 908–0008), was used to determine the $\delta^{18}O$ and δ^2H values of the water samples at the Isotope Hydrology Laboratory of the International Atomic Energy Agency (IAEA) in Vienna and the NNRI of GAEC. Isotopic results were reported on the delta-scale (δ) with respect to Vienna Standard Mean Ocean Water (V-SMOW) (Coplen 1996). The instrument has a precision of approximately 1‰ for δ^2H and 0.2‰ for $\delta^{18}O$. Internal standards were calibrated against the international standards Vienna Standard Mean Ocean Water (VSMOW2) and Standard Light Antarctic Precipitation (SLAP2) for δ^2H and $\delta^{18}O$. Values obtained were normalized using VSMOW2 and SLAP2 on the δ-scale. The internal standards were used as unknowns against certified reference secondary standards from the IAEA to measure the unknown samples. All δ^2H and $\delta^{18}O$ values for water samples were reported based on the VSMOW/SLAP scale.

4 Results

4.1 Hydrochemistry

4.1.1 Rainfall

Proportions of anions in rainfall from the Saltpond station showed the sequence $Cl^- > SO_4^{2-} > NO_3^- > PO_4^{3-} > F^- > Br^- > NO_2^-$, whilst the analogous sequence for the Twifo Praso station was $Cl^- > NO_3^- > SO_4^{2-} > PO_4^{3-} > F^- > Br^- > NO_2^-$. The Cl^- concentrations from the two meteorological stations, Saltpond and Twifo Praso, are shown in Figure 4. The Cl^- anion was the most abundant anion at both stations; Cl^- concentrations from Saltpond station varied between

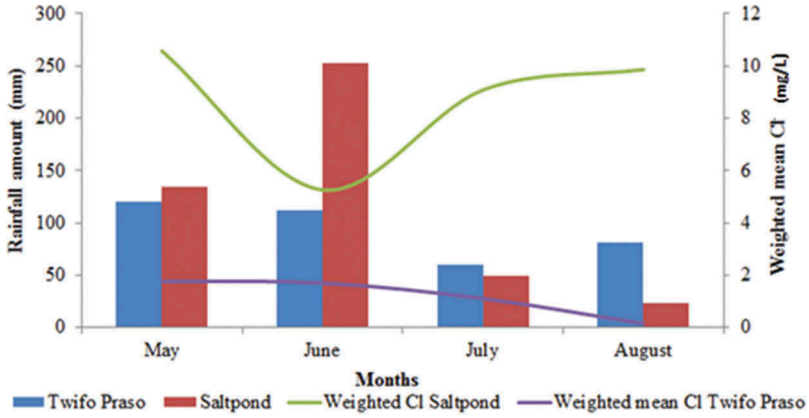

Figure 4. Concentrations of Cl^- in rainfall events between May and August 2010 at the Twifo Praso and Saltpond stations.

1.07 and 22.32 mg/L, with a mean of 9.71 mg/L, while those from Twifo Praso station varied between 0.48 and 8.28 mg/L, with a mean of 3.12 mg/L. Higher values were observed at the Saltpond station closer to the coast, suggesting that the ocean is the major contributor of Cl^- in rainfall.

4.1.2 Shallow groundwaters

A statistical overview of the hydrochemical results of the shallow groundwaters is presented in Table 1(a) (detailed results are presented in the Supplementary material, Table S1). The minimum pH of the shallow groundwaters was 5.2 and occurred in hand-dug well CR4-FZ-03 in the northwestern section of the study area. The maximum pH value of 9.3 occurred in hand-dug well CR4-01 at Ekumfi Asafa in the southern section of the study area close to the Gulf of Guinea (Fig. 2).

Electrical conductivity (EC) of the shallow groundwaters was in the range 540–6050 µS/cm, with a mean of 2102 µS/cm. Elevated EC values in wells CR2-54 (6050 µS/cm) and CR2-53 (5050 µS/cm) occurred at 4 and 16 km from the coast (Fig. 5). The concentration of TDS ranged between 270 and 3030 mg/L, with a mean of 1098 mg/L. The highest TDS of 3030 mg/L occurred in the hand-dug well CR2-54 at Anokye. The dominant cation in the shallow groundwaters was Na^+, followed by Ca^{2+}, Mg^{2+} and K^+. The amount of Na^+ varied from 26.4 to 1430 mg/L. The mean Na^+ content of the shallow groundwaters was 366.9 mg/L. The highest Na^+ concentration (1430 mg/L) occurred in borehole CR2-53 at Abonko and the lowest (26.40 mg/L) in borehole CR4-FZ-14 at Abora Dunkwa. The dominant anion in the shallow groundwaters was Cl^-, followed by HCO_3^- and SO_4^{2-}. The Cl^- in the shallow groundwaters ranged between 39.4 and 2750 mg/L, with a mean of 788 mg/L. Higher concentrations of Cl^- (2750 mg/L) occurred in borehole CR2-54 at Anokye and lower Cl^- was found in borehole CR4-FZ-14 at Abora Dunkwa. Concentrations of NO_3^- varied from 0.15 to 0.18 mg/L, with a mean of 0.15 mg/L. Generally, low NO_3^- concentrations occurred in the shallow groundwaters of the entire study area.

4.1.3 Deep groundwaters

Temperatures of the deep groundwaters were in the 23.2–30.9°C range, with a mean of 28°C. A statistical overview of measured parameters for the deep groundwaters is presented in Table 1(b) (detailed results are in given in the Supplementary material, Table S2). The pH varied from 5.32 to 7.84, indicating slightly acidic to slightly alkaline conditions. A wide variation of EC from 120.6 to 29 000 µS/cm was observed, with a mean of 2347 µS/cm. Higher EC occurred in the deep groundwaters as compared to the shallow groundwaters (Fig. 2). The highest value of 29 000 µS/cm occurred in borehole CR2-45 at Gomoa Abora, which is located 5.9 km from the coast within the amphibolite aquifers (Fig. 2).

The cation Na^+ was the dominant cation in the deep groundwaters. The abundance of cations was in the order $Na^+ > Ca^{2+} > Mg^{2+} > K^+$. The Na^+ concentration varied from 22.2 mg/L in borehole CR4-FZ-08 at Ayeldu to 2770 mg/L in borehole CR2-45 at Gomoa Abora (Fig. 6(a)), with a mean of 335.9 mg/L. The dominant anion in the deep groundwater was Cl^-. The abundance of the anions was in the order $Cl^- > HCO_3^- > SO_4^{2-}$. Concentrations of Cl^- varied from 30.6 mg/L in borehole CR4-FZ-08 at Ayeldu to 4799 mg/L in borehole CR2-49 at Ekumfi Akwakrom (Fig. 6(b)), with a mean of 595.4 mg/L. High values of 1210–4799 mg/L were found in boreholes CR2-23 at Ekumfi Engow, CR2-45 at Gomoa Abora and CR2-49 at Akwakrom (Fig. 6(b)). These values also corresponded to high concentrations of Na^+. The least

Table 1. Statistical summary of hydrochemical data of (a) shallow groundwater and (b) deep groundwater.

Parameter	Temp (°C)	pH	Eh (mV)	EC (µS/cm)	TDS (mg/L)	Salinity (mg/L)	Ca^{2+} (mg/L)	Na^{+} (mg/L)	Mg^{2+} (mg/L)	K^{+} (mg/L)	Cl^{-}(mg/L)	SO_4^{2-}(mg/L)	HCO_3^{-} (mg/L)	NO_3^{-} (mg/L)
(a) Shallow groundwater														
Minimum	26.90	5.20	−104.10	540.00	270.00	300.00	9.34	26.40	8.33	4.45	39.38	20.50	12.20	0.15
Maximum	30.80	9.30	104.50	6050.00	3030.00	3300.00	183.20	1429.50	168.00	468.50	2749.50	184.67	277.53	0.81
Mean	28.54		13.92	2192.00	1097.78	1144.44	68.54	366.93	45.14	83.83	788.00	88.18	141.31	0.51

Parameter	Temp (°C)	pH	Eh (mV)	EC (µS/cm)	TDS (mg/L)	Sal (mg/L)	Ca^{2+} (mg/L)	Na^{+} (mg/L)	Mg^{2+} (mg/L)	K^{+} (mg/L)	Cl^{-}(mg/L)	SO_4^{2-} (mg/L)	HCO_3^{-} (mg/L)	NO_3^{-} (mg/L)
(b) Deep groundwater														
Minimum	23.20	5.32	−36.60	120.60	60.30	100	10.87	22.15	2.88	3.70	30.57	7.46	9.15	0.02
Maximum	30.90	7.84	107.40	29000.00	14420.00	17700	456.70	2769.50	416.70	101.90	4798.50	751.55	780.80	2.26
Mean	27.91		44.16	2346.92	1183.59	1298.57	109.33	335.96	44.76	18.72	595.36	129.09	2.26	0.55

Parameter	F^{-} (mg/L)	PO_4^{3-} (mg/L)	Br^{-} (mg/L)
Minimum	0.00	0.00	0.00
Maximum	0.79	0.51	219.00
Mean	0.31	0.07	41.77

dominant anion in the deep groundwater was SO_4^{2-}, ranging between 7.5 and 751.6 mg/L, with a mean of 129.1 mg/L. The highest SO_4^{2-} concentration of 751.6 mg/L occurred in borehole CR4-04 at Otuam in the aquifer underlain by biotite granite. Extremely low HCO_3^{-} values of 9.2 mg/L occurred further north in the biotite granite and biotite gneiss aquifers further from the coast. The generally low NO_3^{-} concentrations in the study area varied from 0.02 to 2.3 mg/L, with a mean of 0.5 mg/L. Similarly, the concentrations of PO_4^{3-} and F^{-} were low in the entire study area.

4.2 Stable isotope composition of groundwater

Detailed results of the stable isotope compositions of the groundwaters are presented in the Supplementary material, Table S3. Stable isotope compositions of the shallow groundwaters in the study area for $\delta^{18}O$ ranged between −3.09‰ and −1.60‰, with a mean of −2.44‰ and a standard deviation of 0.50 (Supplementary material, Table S4(a)). The stable isotopic composition for $\delta^{2}H$ of shallow groundwater ranged between −12.35‰ and −6.07‰, with a mean of −9.25‰ and a standard deviation of 2.30 (Supplementary material, Table S4 (a)). In deep groundwater, the isotopic composition for $\delta^{18}O$ ranged between −3.07‰ and −1.43‰, with a mean of −2.43‰ and a standard deviation of 0.41 (Supplementary material, Table S4(b)). The $\delta^{2}H$ for deep groundwater ranged between −17.61‰ and −7.04‰, with a mean of −11.99‰ and a standard deviation of 2.73 (Supplementary material, Table S4(b)). The spatial distribution of $\delta^{18}O$ in the study area showed waters with more positive $\delta^{18}O$ inland and more negative $\delta^{18}O$ towards the coast (Fig. 7(a)). The $\delta^{18}O$ and $\delta^{2}H$ data are plotted in Figure 7(b). As revealed in Figure 7(b), the groundwaters are indicative of waters of meteoric origin, i.e. samples close to the Global Meteoric Water Line (GMWL) and Local Meteoric Water Line (LMWL). Shallow and deep groundwaters show similar isotopic compositions suggesting a hydraulic connection between shallow groundwater and deep groundwater as observed from the chemical data. This implies deep groundwater is recharged vertically from the unsaturated soil zone.

5 Discussion

5.1 Hydrochemistry

Shallow and deep groundwater in the study area exhibited similar sequences of abundance of cations and anions signifying a hydraulic connection between them. The highest EC of 29 000 µS/cm in borehole CR2-45 at

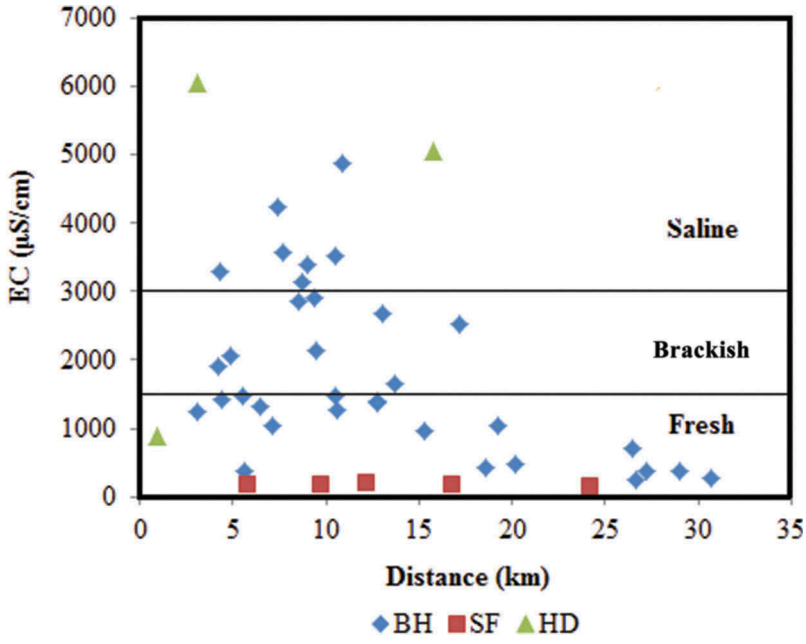

Figure 5. Distribution of EC levels of the groundwater with distance from the coast. The classification of the waters into fresh, brackish and saline is based on the scheme employed by Park *et al.* (2012).

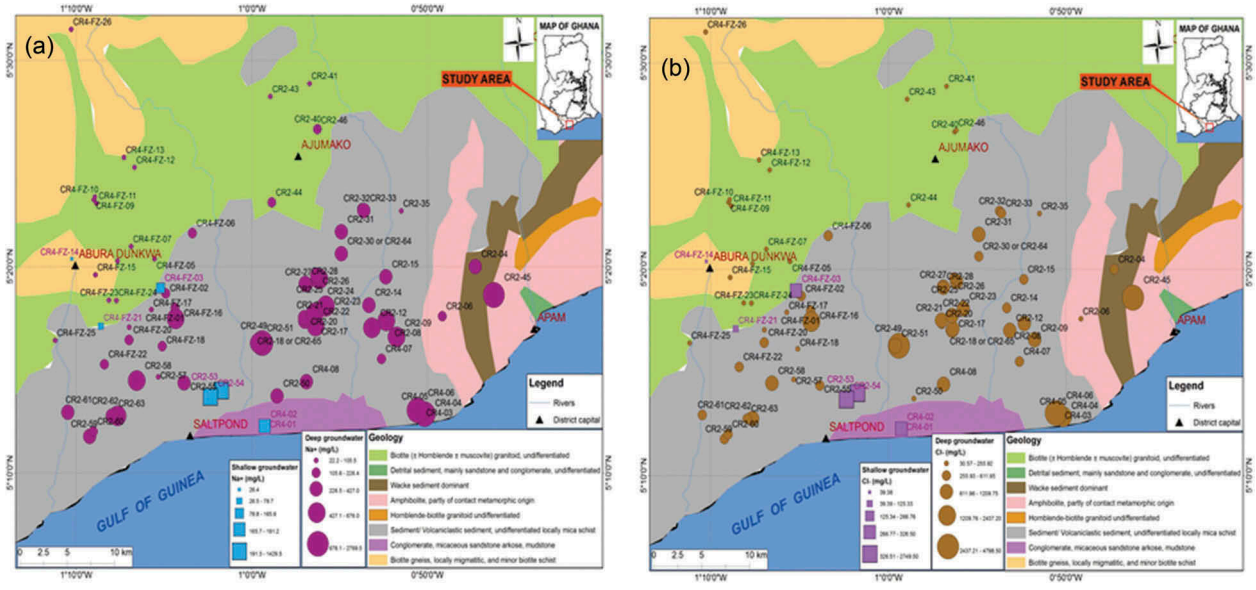

Figure 6. Spatial distribution of (a) Na^+ and (b) Cl^- with respect to the geology of the area.

Gomoa Abora can be explained by the proximity of the coast, and also by weathering of minerals of the rocks in the area. Park *et al.* (2012) evaluated the relationship between EC levels and distance from the coast in South Korean aquifers and observed negative correlation in alluvial coastal aquifers, but no correlation in bedrock coastal aquifers. They developed a classification scheme to describe the quality of water in South Korea. Groundwaters with EC < 1500 µS/cm were classified as "fresh", those having EC within the range 1500–3000 µS/cm were classified as "brackish", and those with EC levels >3000 µS/cm were described as "saline". Plotting of EC values in the Ochi-Narkwa basin against distance from the coast (Fig. 5) reveals a weak negative correlation ($r = -0.41$), implying that salinity does not depend on distance from the coast. According to the classification scheme of Park *et al.* (2012), Figure 5 shows that some boreholes within 7 km of the coast had EC of 100–1000 µS/cm and, therefore, can be classified as fresh. Some boreholes and hand-dug wells within the same distance from the coast

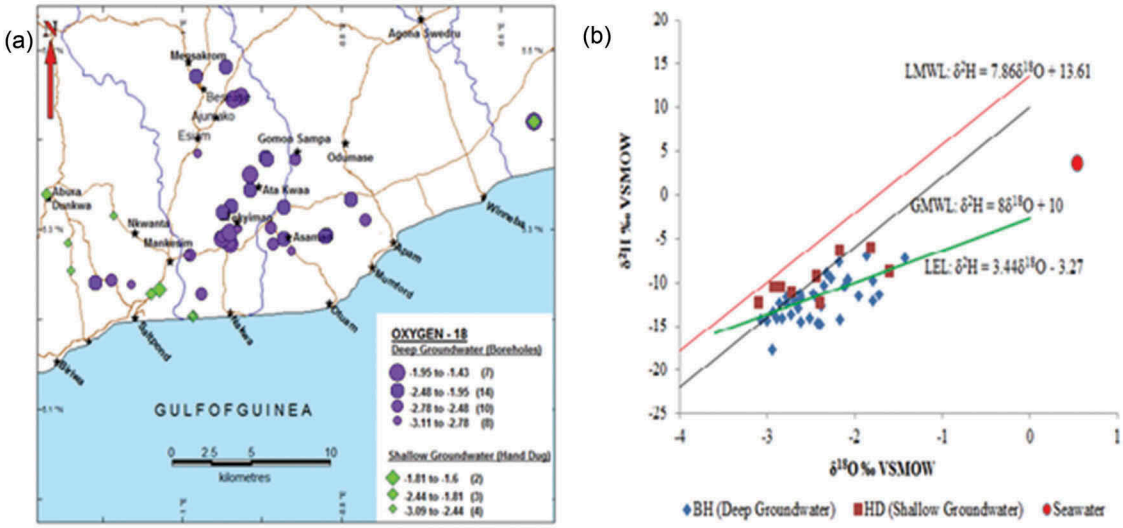

Figure 7. (a) Spatial distribution of $\delta^{18}O$ in the study area. (b) Relationship between $\delta^{2}H$‰ V-SMOW and $\delta^{18}O$‰ V-SMOW for shallow and deep groundwater.

had EC above 1000 µS/cm and therefore they are saline. From 7 km to about 15 km from the coast, some boreholes had an EC below 1000 µS/cm, indicating freshwater. Similar observations can be made in Figure 2, which shows the spatial distribution of EC with respect to the geology of the study area. The origin of the electrical conductivities in the area is complex, indicating weathering of rocks, seawater intrusion, sea aerosol spray, halite dissolution and slow movement of groundwater in the area. Of the deep groundwaters, 59% had EC < 1500 µS/cm and 41% had EC > 1500 µS/cm. Figure 2 indicates the possible groundwater flow direction from the inland areas in the north with low EC values towards the coast in the south with increasing EC. This agreed with the flow direction obtained in Figure 3 from hydraulic heads.

The cations Na^+, Ca^{2+}, Mg^{2+} and K^+ are significant constituents of silicate rocks (Freeze and Cherry 1979) and hence Na^+ in groundwater in the Ochi-Narkwa basin is considered to originate from silicate weathering. A secondary source of Na^+ is halite, concentrated in the soil zone by evaporation and leached into the groundwater by infiltrating rain. The Ca-feldspars ($CaAl_2Si_2O_8$) are considered the main source of calcium, releasing Ca^{2+} in the presence of carbonic acid (H_2CO_3) generated in the soil zone. Other possible sources of Ca^{2+} in the groundwaters include dissolution of the mineral hornblende [$Ca_2(MgFeAl)_5(AlSi)_8O_{22}$] and pyroxenes. The Mg^{2+} in groundwater probably comes from biotite [$K(Mg,Fe)_3(AlSi_3)O_{10}(OH,F)_2$] and hornblende, which are constituents of the aquifers in the study area. Micas (muscovite and biotite) are major constituents of the sediment/volcaniclastic sediment in the area and therefore responsible for K^+ in the groundwater.

Generally, Cl^- is not a significant constituent of silicate rocks. The presence of Cl^- in groundwater is usually attributed to atmospheric sources, decomposition of organic matter and trace impurities in rocks and minerals (Freeze and Cherry 1979). It may also result from seawater encroachment and intrusion due to proximity to the coast. Like Cl^-, SO_4^{2-} is not a major constituent of silicate rocks and therefore its content in the study area is low. The elevated SO_4^{2-} concentration of 751.6 mg/L in the biotite granite aquifer may be explained by oxidation of pyrite observed in the rocks of the area. Very low NO_3^- concentrations may be attributed to less vigorous anthropogenic activities in the area. Low F^- and PO_4^{3-} concentrations in deep groundwater may be attributed to lack of phosphate minerals and fluorites in the rocks of the study area. Elevated concentrations of F^- in groundwater in Northern Ghana, however, are attributable to the dissolution of the mineral fluorite in the rocks (Apambire 1997).

5.2 Hydrochemical facies

The Piper (1944) trilinear plot of shallow unconfined groundwaters showed two main water types: NaCl and non-dominant (mixed) (Fig. 8(a)). In the case of deep confined groundwater, four main water types were identified (Fig. 8(b)): Ca-Mg-HCO_3, labelled I; NaCl, labelled II; Ca-Mg-Cl-SO_4, labelled III; non-dominant, labelled IV. The groundwater evolved from a Ca-Mg-HCO_3 water type (freshwater) in a recharge area to a NaCl water type (saline), indicating a discharge area. A general flow direction is thus shown in Figure 8(b)

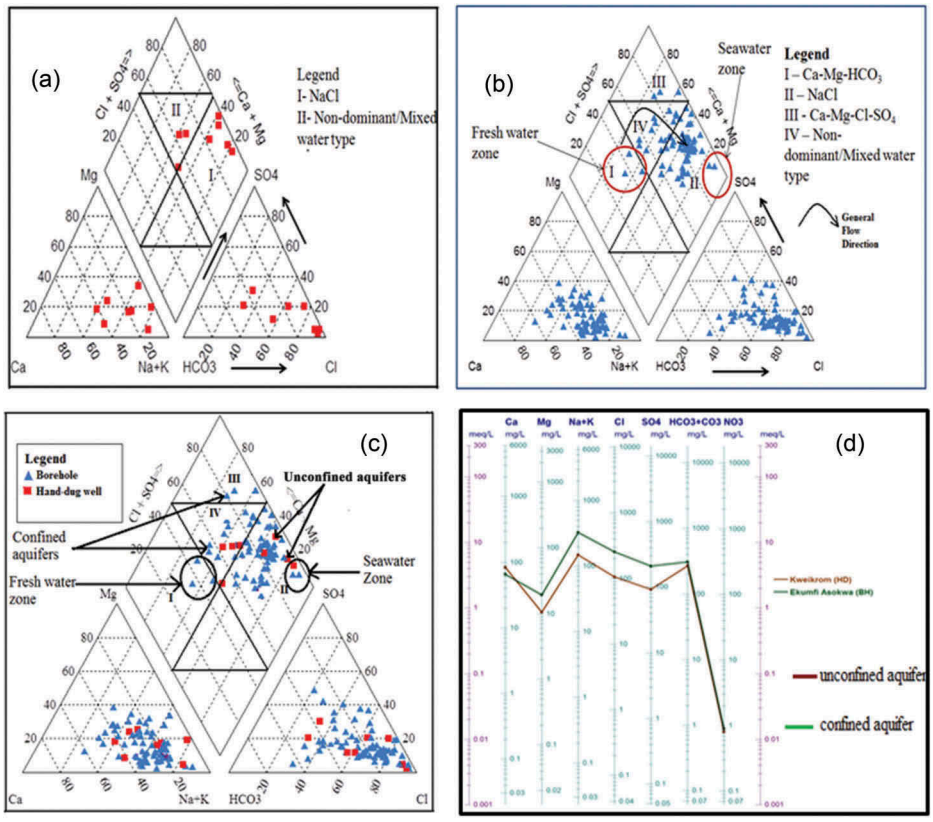

Figure 8. Hydrochemical facies in the study area using the Piper (1944) trilinear diagram for (a) shallow unconfined groundwater, (b) deep confined groundwater, and (c) unconfined and confined groundwater plotted together; (d) Scholler diagram showing the relationship between unconfined and confined groundwater.

from inland (freshwater zone) to the coast (saline zone), as observed in Figure 3. One shallow and two deep groundwater samples located near the seawater zone of the Piper trilinear diagram in Figure 8(c) indicate that they have been affected by seawater intrusion. Generally, the most common hydrochemical facies in both shallow unconfined and deep confined groundwaters is NaCl. The Schoeller diagram in Figure 8(d) is used to explain the relationship between unconfined and confined aquifers in the study area. Although both aquifers have similar hydrochemical patterns, the confined aquifers are more mineralized than the unconfined aquifers. This may be explained by lower transmissivities observed in confined aquifers in the area, which in turn result in slow movement and longer transit times of groundwater. The spatial distribution of the various water types in Figure 9 shows that NaCl waters predominantly occur in the mica schist and in part of the biotite granite aquifers.

5.3 Origin of salinity in the groundwaters

The ocean is a major source of aerosols and gases for the overlying atmospheric boundary layer. Bubbles produced by waves breaking from the ocean burst after rising back to the air–sea interface and produce seasalt aerosols (Keene *et al.* 1986). The seasalt aerosols produced are removed from the atmosphere by precipitation. The chemistry of precipitation thus becomes dominated by marine components (Keene *et al.* 1986). The various ionic species contributing to seasalt in the Ochi-Narkwa study area were calculated using linear regression techniques based on three major assumptions:

(1) all reference species are contributed by seasalt;
(2) no fractionation occurs during formation of the aerosol; and
(3) no fractionation occurs during atmospheric transport and scavenging.

If the species of interest are contributed solely by seasalt, a regression of the concentrations of the species of interest and reference species yields a slope approximately equal to the seawater ratio and intercept approximately equal to zero. A slope that differs from the seawater ratio and an intercept that differs from zero are indications of a non-seasalt contribution. Keene *et al.* (1986) calculated various

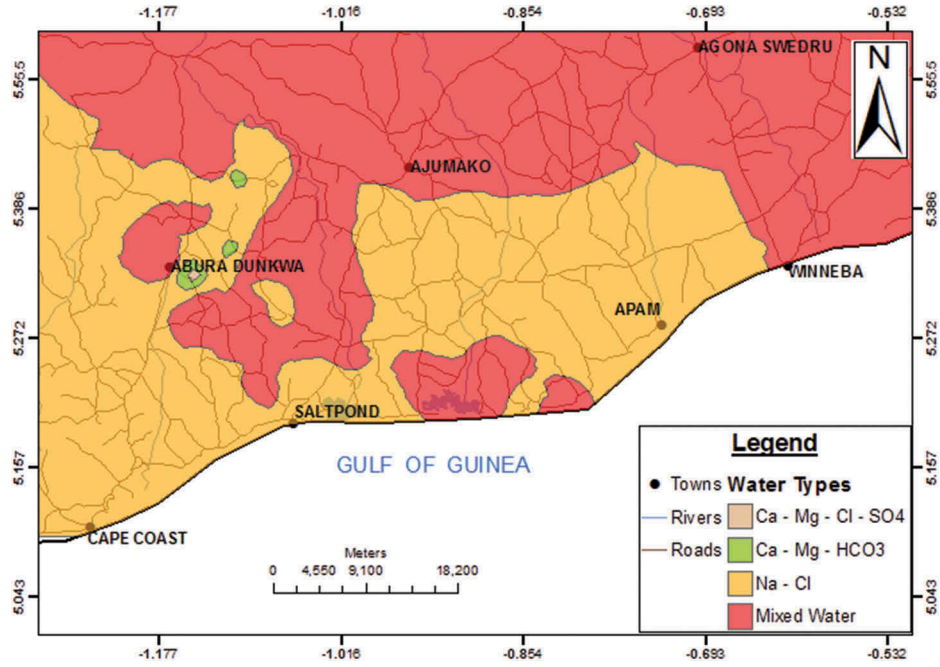

Figure 9. Spatial distribution of water types in the study area.

ionic ratios in seasalt including the Na/Cl ratio and found them to be 0.86. This ratio has been employed widely to determine the origin of salinity in groundwater (De Montety *et al.* 2008, Al-Charideh 2011, Cheong *et al.* 2011). Groundwater having a Na/Cl molar ratio equal to 0.86 is considered to have originated from seasalt or seawater and halite dissolution.

The plot of Na^+ against Cl^- concentrations in groundwater in the study area (Fig. 10(a)) shows a strong correlation of 0.93, indicating most likely a common source of saline water. The Na–Cl relationship in Figure 10(a) and (b) shows most of the samples along the 1:1 line, indicating that the sources of Na^+ and Cl^- in the groundwater may originate from seasalt aerosols, direct seawater intrusion and halite dissolution. The geology of the area does not indicate halite deposits. It is therefore supposed that halite, originating from high concentrations of Cl^- in rainfall (Fig. 4), accumulated over time in the soil zone by evaporation and was flushed into the groundwater zone by infiltrated rainwater. The Na/Cl molar ratios of the groundwaters ranged from 0.36 to 5.18, and 83% of the samples have a Na/Cl molar ratio equal to 1, suggesting that halite dissolution is a major hydrogeochemical process in the area. A ratio equal to 1 implies that halite dissolution is responsible for contributing Na^+ ions and a ratio greater than 1 means that silicate weathering would contribute to Na^+ ions in the groundwater (Singh *et al.* 2011). In this study, 14% of the samples have a Na/Cl molar ratio greater than 1, indicating silicate weathering. This is further confirmed by the plot of TDS against Na/Na+Ca (Fig. 10(c)), as proposed by (Singh *et al.* 2011), where most of the samples are plotted in the rock dominance region, accounting for a weathering origin. Three percent of the samples have Na/Cl molar ratio less than 1 and suggest possible seawater intrusion.

These findings were further examined using the Br^-/Cl^- ratio as a reliable indicator of the origin of salinity due to its specific composition in various saline sources (Vengosh *et al.* 2005, De Montety *et al.* 2008, El-Fiky 2010). The Br^-/Cl^- ratio of seawater observed by Helstrup *et al.* (2007) in parts of Ghana and Togo close to the Gulf of Guinea was 0.0035 ± 0.0002 (weight ratio). The Br^-/Cl^- ratios of the groundwaters in the Ochi-Narkwa basin ranged from 0.0054 to 2.075. Four of the boreholes (CR2-01 at Kweikrom, CR2-22 at Ekumfi Techiman, CR2-23 at Ekumfi Engow and CR2-45 at Gomoa Abora) are plotted close to the seawater line and therefore show characteristics of seawater transgression into groundwater, sea aerosol spray or halite dissolution (Fig. 10(d)). The remaining samples occur above the Br^-/Cl^- ratio for seawater, suggesting salinity sources other than seawater intrusion. However, Figure 10(d) reveals a general decrease in Br^-/Cl^- ratio with increasing Cl^- concentration, as shown by the arrow AB, suggesting a tendency to seawater characteristics.

The SO_4^{2-}/Cl^- ratio was also used to investigate a possible seawater intrusion. Marie and Vengosh (2001)

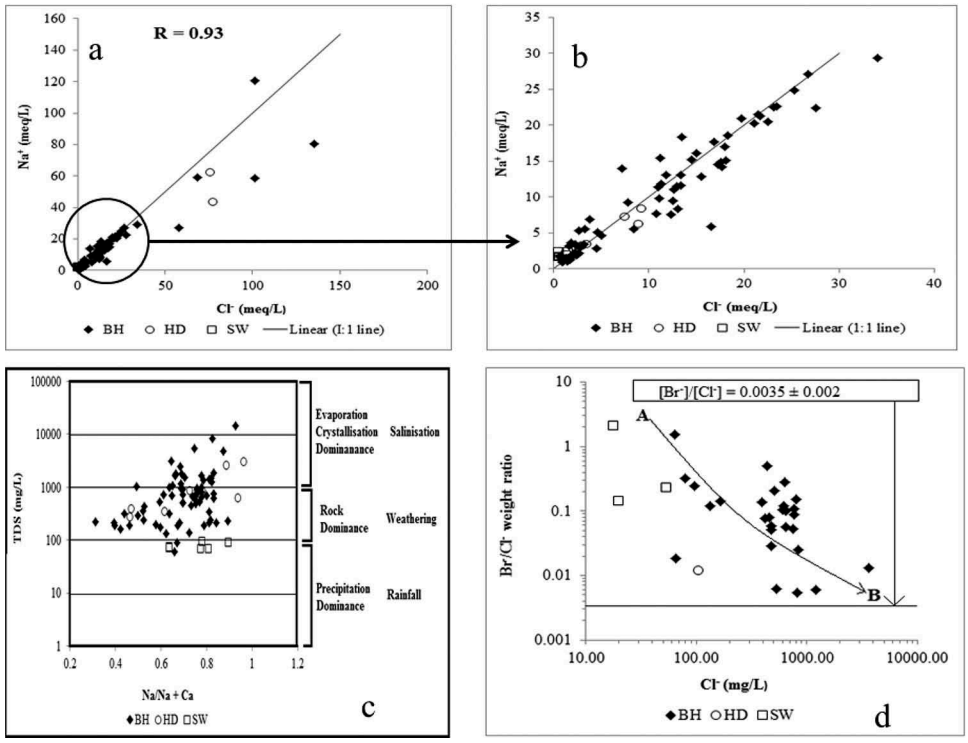

Figure 10. (a) and (b) Na–Cl relationship of groundwater in the coastal areas of the Central Region. (c) Scatter plot between TDS and Na/(Na+Ca) showing rock-dominant weathering in the area (after Singh *et al.* 2011). (d) Br^-/Cl^- weight ratio *vs* Cl^- (mg/L).

recorded a seawater ratio for SO_4^{2-}/Cl^- of 0.15; a ratio greater than 0.15 indicates additional SO_4^{2-} input from fertilizer application, leaching of contaminated landfill or oxidation of sulphides (Marie and Vengosh 2001). A plot of SO_4^{2-} against Cl^- from the Ochi-Narkwa study area shows a moderate positive correlation of 0.62 (Fig. 11(a)). SO_4^{2-}/Cl^- ratios for samples collected in the study area ranged between 0.02 and 4.09. Of the samples, 68% had SO_4^{2-}/Cl^- ratios above the seawater value, indicating additional sources of SO_4^{2-} into the groundwater system (Fig. 11(b)); 32% had SO_4^{2-}/Cl^- ratios either equal to or less than the seawater value, hence showing characteristics of seawater origin.

In Figure 7(b) both shallow and deep groundwaters deviate from the GMWL and the LMWL. The groundwater regression line is defined by the equation $\delta^2H = 3.44\delta^{18}O - 3.27$. A regression line of slope 3.44 suggests either evaporation from the soil zone before recharge to the aquifers or mixing of shallow groundwater and deep groundwater. Deviation from the GMWL and LMWL with a slope of less than 8 provides evidence of evaporation from the soil zone. The depths to water levels in the study area support this assertion. The depths to water levels, as indicated in Section 2, varied between 0 and 20 m below the land surface with an average of 5.8 m. The borehole depths (bottom of borehole) in the area were 18–94.5 m, with a mean of 34.5 m. The depths to water levels show that groundwater is accessed close to the surface. For the shallow groundwaters the depths ranged between 6 and 12 m. Both shallow and deep groundwaters have similar hydrochemical facies and similar $\delta^{18}O$ and δ^2H compositions, implying recharge from the shallow groundwater to deep groundwater via a preferential path. This exhibits mixing of shallow groundwater and deep groundwater, hence the mixing line.

The majority of the boreholes have been constructed at depths closer to the surface and are therefore affected by evaporation. Salt layers in the unsaturated zone are therefore possible. The effect of a possible seawater intrusion was also investigated by plotting Cl^- against $\delta^{18}O‰$ (Fig. 12), which showed no significant relationship between the parameters. Figure 12 depicts that there is no distinct change in $\delta^{18}O‰$ with increasing Cl^- concentration, implying that salinity originates dominantly from dissolution of salts from soils and rocks. This explains why the majority of the groundwaters are located in the dissolution band of the diagram. Two boreholes appear in the mixing band, suggesting

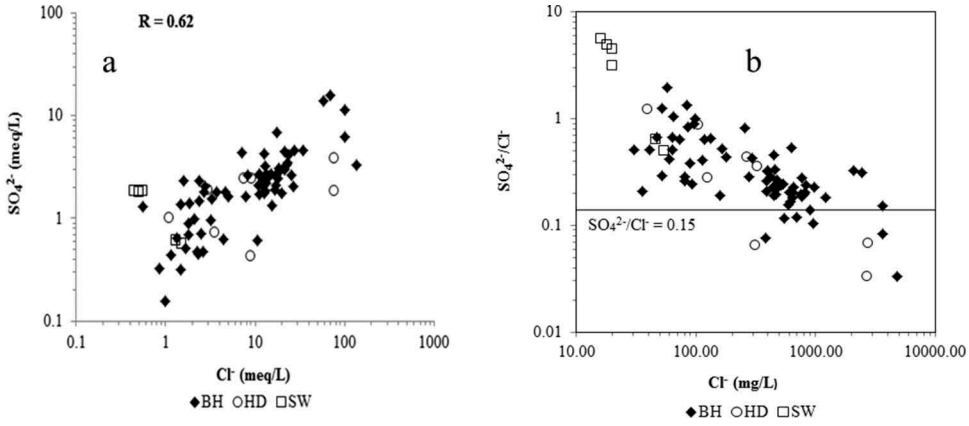

Figure 11. (a) SO_4^{2-} (meq/L) *vs* Cl^- (meq/L), and (b) SO_4^{2-}/Cl^- *vs* Cl (mg/L) .

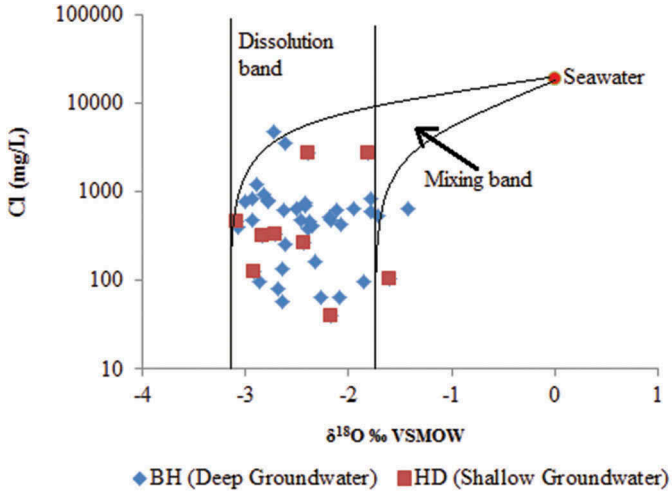

Figure 12. Relationship between Cl (mg/L) and $\delta^{18}O$‰ V-SMOW.

seawater intrusion. One of the hand-dug wells shows elevated Cl^- concentration as a result of evaporation.

The Cl^- concentration data from four soil profiles (Fig. 13) in the vicinity of Ekumfi Akwakrom near Ekumfi Asokwa were used to assess the presence of Cl^- in the unsaturated soil. The Cl^- profiles displayed large variations in Cl^- concentration: low concentrations of 50 mg/kg occurring between 20 and 60 cm and higher concentrations (99.9–449.8 mg/kg) between 80 and 120 cm below the surface (Fig. 13). All measured Cl^- profiles are bulge shaped, with decreasing Cl^- concentrations below the bulge at depth. The upper parts of profiles 1, 3 and 4 reveal a constant Cl^- value of 49.9 mg/kg, indicating a period of non-deposition of Cl^-, or that Cl^- may have been leached to deeper zones of the profiles and eventually to the saturated zone (Fig. 13(a), (c) and (d)). In the case of Profile 2 (Fig. 13(b)), a minor Cl^- peak occurs at the upper part of the profile (49.9 mg/kg), and a major Cl^- peak occurs at 140 cm (249.2 mg/kg). Thus, Cl^- had probably already accumulated in this zone over time. The lower Cl^- values below 140 cm depth indicate that Cl^- is being dissolved and leached to deeper horizons. Minor peaks are observed between 20 and 100 cm. The Cl^- peaks show periods of maximum accumulation in the unsaturated soil zone. It can be concluded that NaCl zones occur in lenses and support the existence of salt crusts at different depths, notably between 80 and 120 cm, and therefore that dissolution of these salts in the soil zone contributes to the high salinity in the groundwaters, as revealed by results from both geochemical and stable isotopic considerations.

The $\delta^{13}C$ of total dissolved inorganic carbon (TDIC) of groundwater was employed to further investigate possible seawater intrusion processes. As the geology of the area does not contain carbonate rocks, carbonate minerals could only occur by

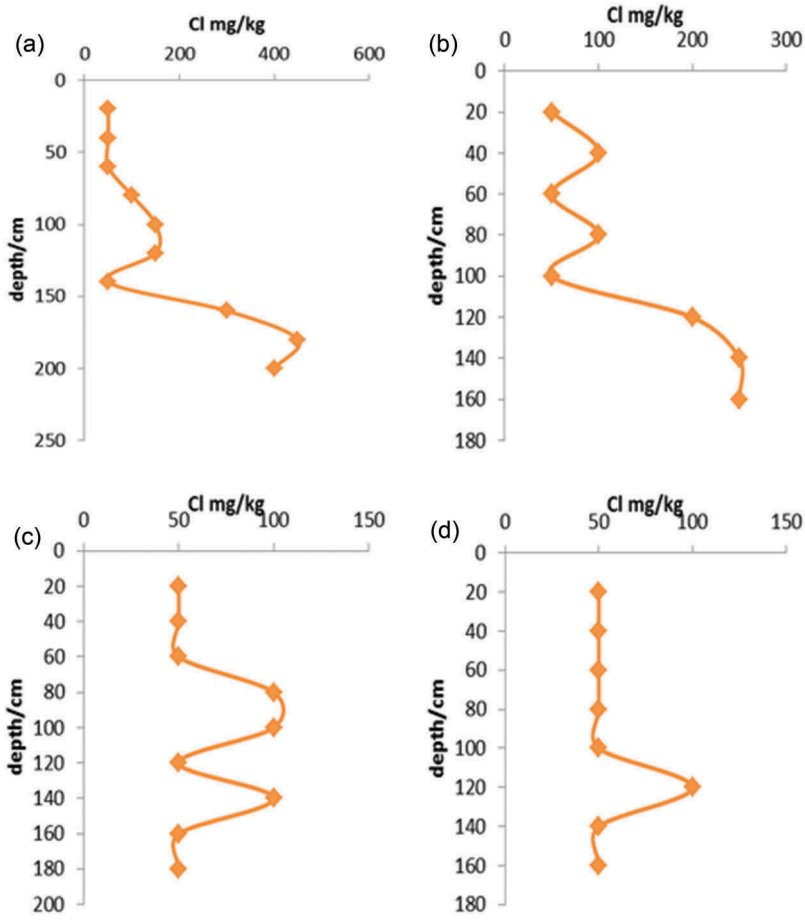

Figure 13. Variation of Cl^- (mg/kg) concentration in the unsaturated soil zone with depth (cm) .

secondary mineralization. It is therefore assumed that $\delta^{13}C$ of seawater is unlikely to be affected by geochemical reactions and thus be conserved for tracing of seawater intrusion in the groundwaters in the study area.

Carbon-13 ($\delta^{13}C$) content of seawater usually varies from –2 to 2‰ V-PDB. In the Mediterranean Sea, Yechieli *et al.* (2001) reports a value of 0‰ V-PDB. The $\delta^{13}C$ for the ocean is quoted as 0‰ V-PDB, while that of groundwater ranges from 0‰ to –20‰ V-PDB (Clark and Fritz 1997). If groundwater was intruded by seawater, $\delta^{13}C$ values would be close to those of the ocean or show $\delta^{13}C$ enrichment towards the value of the ocean. Carbon-13 of groundwater in the study area varied from –19.30 to –7.94‰ V-PDB, with a mean of –14.56‰ V-PDB. The groundwaters in the study area are more depleted in $\delta^{13}C$ compared to the ocean. Applying $\delta^{13}C$‰ V-PDB as an indicator of seawater intrusion to coastal aquifers, $\delta^{13}C$ values of saline groundwater and non-saline groundwater are plotted against chloride concentrations in mg/L. If seawater intrusion is the cause of salinity of groundwater, an increase in Cl^- concentration of groundwater with a corresponding enrichment of $\delta^{13}C$ content of groundwater will occur. A plot of $\delta^{13}C$ against Cl^- (mg/L) for 24 groundwater samples in the study area reveals no such correlation (r = 0.07), indicating that the samples are not of a common source (Fig. 14). It can also be deduced from Figure 14 that $\delta^{13}C$ becomes more depleted with increasing Cl^- concentration. This indicates that the significant component of the dissolved inorganic carbon (DIC) in the Ochi-Narkwa basin is not derived from marine sources, but rather from biogenic sources. This indicates that groundwater salinization may not be as a result of seawater intrusion.

5.4 Conceptual flow model of the study area

A conceptual flow model showing the mechanism of salinization in the study area has been proposed (Fig. 15). It reveals that groundwater flows

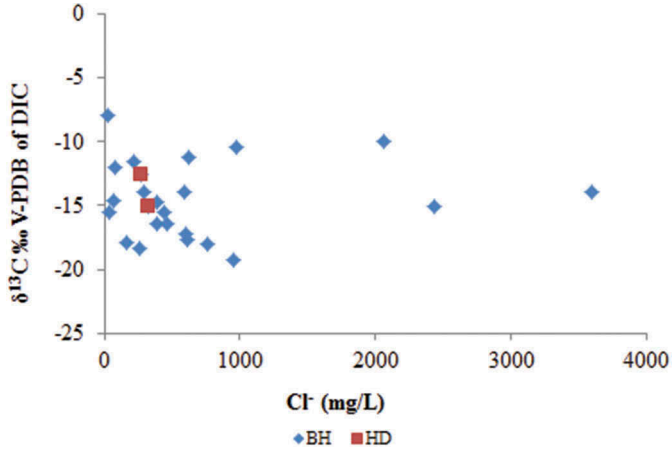

Figure 14. Plot of $\delta^{13}C$ (‰) *versus* V-PDB against Cl^- (mg/L) in the Central Region.

dominantly from the northwestern section (inland) of the study area to the southeastern section (towards the coast). Evaporation over the sea surface results in the formation of suspended particles in the atmosphere referred to as sea aerosols, mostly rich in NaCl. The aerosols are deposited on the ground surface. Rain infiltrating into the soil dissolves the salts on the surface, which are precipitated as lenses of salt crust in the unsaturated soil zone. These salts are later leached into the groundwater, causing salinization of groundwater as demonstrated in Figure 15. Rock weathering also accounts for salinization of groundwater in the study area.

6 Summary and conclusion

Anion chemistry of rainfall showed a higher Cl^- concentration at the coast than inland. Shallow and deep groundwaters showed similar hydrochemical patterns, dominated by Na^+ and Cl^-. Cation concentrations occurred in the order $Na^+ > Ca^{2+} > Mg^{2+} > K^+$ and the anions in the order $Cl^- > HCO_3^- > SO_4^{2-}$. The major hydrochemical facies of the shallow groundwater was Na-Cl and the major facies of the deep groundwater were Ca-Mg-HCO_3, Na-Cl, Ca-Mg-Cl-SO_4 and non-dominant water types. Of the deep groundwaters, 59% had EC < 1500 and 41% had EC > 1500 µS/cm. A conceptual model of groundwater flow and processes of groundwater

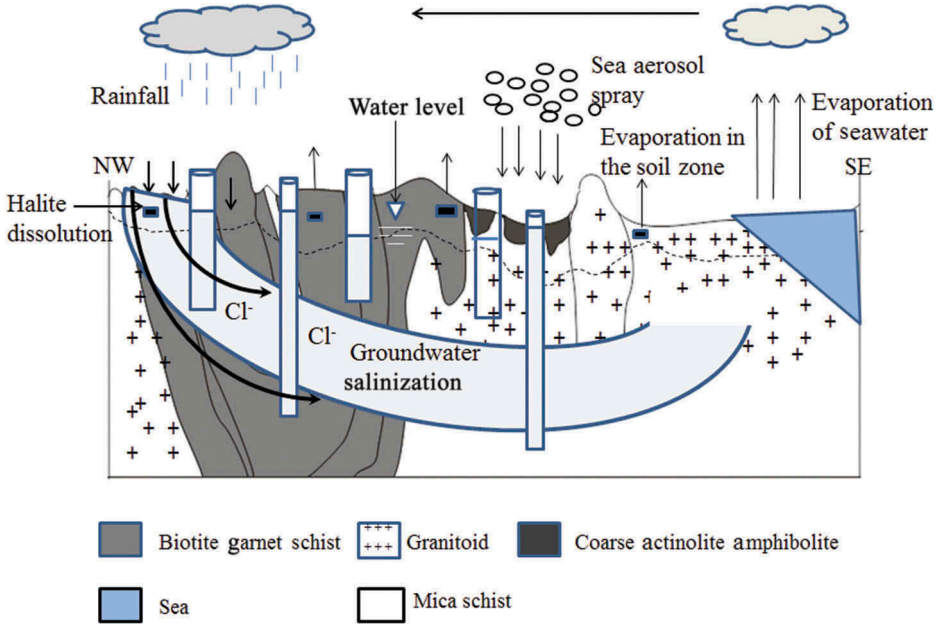

Figure 15. Conceptual flow model explaining the mechanism of salinization in the study area (modified from Geological Survey field sheet no. 32).

salinization was developed. Groundwater flow was hypothesized from the inland areas (northwestern section of the area) towards the coast (southeastern section). Elevated EC in the study area was attributed to the impervious nature of the rocks, which results in longer contact time with the rocks, slow groundwater movement and therefore a greater amount of dissolved minerals.

The Na/Cl molar ratio within the range 0.36–5.18 revealed that the principal source of high groundwater salinity is halite dissolution, because 83% of the samples had ratios equal to 1. Fourteen percent had ratios greater than 1, suggesting that silicate weathering or rock dissolution contributed to the salinity sources. Three percent of the groundwater samples showed characteristics of seawater intrusion. These findings were also supported by the analysis of Br^-/Cl^- ratio *versus* Cl, the ratio SO_4^{2-}/Cl^- and the Cl^-–$\delta^{18}O$ relationship.

The Cl^- concentrations in the unsaturated soil zone indicated the occurrence of NaCl salt crusts at different depths, notably between 80 and 120 cm. The $\delta^{13}C$–Cl^- relationship indicated no impact of seawater intrusion.

The overall assessment of groundwater in the study area revealed a strong geological background to the major ion hydrochemistry in the coastal zone of Central Ghana with no significant seawater intrusion.

Acknowledgements

We thank the staff of the isotope hydrology and the inorganic laboratories for analysing the samples, in particular Nash Bentle, Eunice Agyeman, Ruby Torto and Godfred Anyanu. The Community Water and Sanitation Agency (CWSA), Central Region, is acknowledged for providing existing hydrogeological and hydrochemical data on boreholes.

Disclosure statement

No potential conflict of interest was reported by the authors.

Funding

This research work is based on the technical cooperation project GHA/8009 supported by the International Atomic Energy Agency (IAEA). We would also like to thank the National Nuclear Research Institute (NNRI) of the Ghana Atomic Energy Commission (GAEC) for their financial and logistic support in conducting this study [GHA/8009].

References

Al-Charideh, A., 2011. Geochemical and isotopic characterization of groundwater from shallow and deep limestone aquifers system of Aleppo basin (north Syria). *Environmental Earth Sciences*, 65, 1157–1168. doi:10.1007/s12665-011-1364-6

Apambire, W.B., 1997, Geochemistry, genesis, and health implications of fluoriferous groundwaters in the upper regions of Ghana. *Environmental Geology*, 33 (1), 13-24.

Armah, T., 2002. *Hydrochemical and geophysical studies of groundwater salinity, Central Region, Ghana*. Thesis (PhD). University of Ghana.

Boghici, R., 2003. *A field manual for groundwater sampling, user manual 51 [online]*. TX: Texas Water Development Board. Available from: http://www.twdb.texas.gov/publications/reports/manuals/UM-51/FieldManual.pdf. [Accessed 18 November 2016].

Bouchaou, L., *et al.*, 2008. Application of multiple isotopic and geochemical tracers for investigation of recharge, salinization, and residence time of water in the Souss–Massa aquifer, southwest of Morocco. *Journal of Hydrology*, 352, 267–287. doi:10.1016/j.jhydrol.2008.01.022

Cheong, J.Y., *et al.*, 2011. Groundwater nitrate contamination and risk assessment in an agricultural area, South Korea. *Environmental Earth Sciences*, 66, 1127–1136. doi:10.1007/s12665-011-1320-5

Clark, I.D., and Fritz, P., 1997. *Environmental isotopes in hydrogeology*. Boca Raton, FL: CRC Press.

Coplen, T.B., 1996. New guidelines for reporting stable hydrogen, carbon, and oxygen isotope-ratio data. *Geochimica et Cosmochimica Acta*, 60 (17), 3359–3360. doi:10.1016/0016-7037(96)00263-3

De Montety, V., *et al.*, 2008. Origin of groundwater salinity and hydrogeochemical processes in a confined coastal aquifer: case of the Rhône delta (Southern France). *Applied Geochemistry*, 23, 2337–2349. doi:10.1016/j.apgeochem.2008.03.011

El-Fiky, A.A., 2010. Hydrogeochemical characteristics and evolution of groundwater at the Ras Sudr-Abu Zenima Area, Southwest Sinai, Egypt. *JKAU: Earth Sciences*, 21 (1), 79–109. doi:10.4197/Ear.21-1.4

Freeze, R.A. and Cherry, J.A., 1979. *Groundwater prentice*. Englewood Cliffs, NJ: Englewood Cliffs.

Helstrup, T., Jørgensen, N.O., and Banoeng-Yakubo, B., 2007. Investigation of hydrochemical characteristics of groundwater from the Cretaceous-Eocene limestone aquifer in southern Ghana and southern Togo using hierarchical cluster analysis. *Hydrogeology Journal*, 15, 977–989. doi:10.1007/s10040-007-0165-1

Hirdes, W., Davis, D.W., and Eisenlohr, B.N., 1992. Reassessment of Proterozoic granitoid ages in Ghana on the bases of U/Pb zircon and monazite dating. *Precambrian Research*, 56 (1–2), 89–96. doi:10.1016/0301-9268(92)90085-3

IAEA (International Atomic Energy Agency), 2008. *Field estimation of soil water content––A practical guide to methods, instrumentation and sensor technology*. Vienna: IAEA-TCS-30. ISSN 1018–5518.

Jørgensen, N.O. and Banoeng-Yakubo, B.K., 2001. Environmental isotopes (^{18}O, ^{2}H, $^{87}Sr/^{86}Sr$) as a tool in groundwater investigations in the Keta Basin, Ghana. *Hydrogeology Journal*, 9 (2), 190–201. doi:10.1007/s100400000122

Keene, W.C., *et al.*, 1986. Seasalt corrections and interpretation of constituent ratios in marine precipitation. *Journal of Geophysical Research*, 91 (6), 6647–6658. doi:10.1029/JD091iD06p06647

Kim, Y., *et al.*, 2003. Hydrogeochemical and isotopic evidence of groundwater salinization in a coastal aquifer: a case study in

Jeju volcanic island, Korea. *Journal of Hydrology*, 270 (3–4), 282–294. doi:10.1016/S0022-1694(02)00307-4

Kortatsi, B.K., 2006. Hydrochemical characterization of groundwater in the Accra plains of Ghana. *Environmental Geology*, 50 (3), 299–311. doi:10.1007/s00254-006-0206-4

Kortatsi, B.K., 1994. Groundwater utilization in Ghana. *In*: J. Soveri and T. Suokko, eds. Proceedings of the helsinki conference on groundwater resources at risk, Helsinki, Finland. Vol. 222. Wallingford, UK: International Association of Hydrological Sciences, IAHS Publ, 149–156.

Leube, A., *et al*., 1990. The early proterozoic birimian supergroup of Ghana and some aspects of its associated gold mineralization. *Precambrain Research*, 46, 139–165. doi:10.1016/0301-9268(90)90070-7

Marie, A. and Vengosh, A., 2001. Sources of salinity in groundwater from Jericho Area, Jordan Valley. *Groundwater*, 39 (2), 240–248. doi:10.1111/gwat.2001.39.issue-2

Obuobie, E. and Barry, B., 2010. *Groundwater in sub-Saharan Africa: implications for food security and livelihoods. Ghana Country Status on Groundwater* [online]. Final Report, International Water Management Institute, 48. Available from: http://gwafrica.iwmi.org/Data/Sites/24/media/pdf/Country_Report-Ghana.pdf [Accessed 17 November 2016].

Park, Y., *et al*., 2012. National scale evaluation of groundwater chemistry in Korea coastal aquifers: evidences of seawater intrusion. *Environmental Earth Sciences*, 66, 707–718. doi:10.1007/s12665-011-1278-3

Piper, A.M., 1944. A graphic procedures in the geochemical interpretation of water analyses. *American Geophysical Union Trans*, 25, 914–923. doi:10.1029/TR025i006p00914

Singh, C.K., Shashtri, S., and Mukherjee, S., 2011. Integrating multivariate statistical analysis with remote sensing and GIS for geochemical assessment of groundwater quality: a case study of Rupnagar district in Shiwaliks of Punjab. *Environmental Earth Sciences*, 62 (7), 1387–1405. doi:10.1007/s12665-010-0625-0

Taylor, P.N., *et al*., 1992. Early Proterozoic crustal evolution in the Birimian of Ghana: constraints from geochronology and isotope geology. *Precambrian Research*, 56, 97–111. doi:10.1016/0301-9268(92)90086-4

Vengosh, A., *et al*., 2005. Sources of salinity and boron in the Gaza Strip: National contaminant flow in southern Mediterranean coastal aquifer. *Water Resources Research*, 41, W01013. doi:10.1029/2004WR003344

Yechieli, Y., *et al*., 2001. Radiocarbon in seawater intruding into the Israeli Mediterranean coastal aquifer. *Radiocarbon*, 43, 773–781.